A multispecies BCO2 beak color polymorphism in the Darwin's finch radiation

Enbody, Erik; Sprehn, C. Grace ; Abzhanov, Arhat; Bi, Huijuan; Dobreva, Mariya P; Osborne, Owen; Rubin, Carl-Johan ; Grant, Peter; Grant, B. Rosemary; Andersson, Leif

Current Biology

DOI:
10.1016/j.cub.2021.09.085

Published: 22/10/2021

Peer reviewed version

A multispecies *BCO2* beak color polymorphism in the Darwin's finch radiation

Erik D. Enbody[1*], C. Grace Sprehn[1], Arhat Abzhanov[2], Huijuan Bi[1], Mariya P. Dobreva[2], Owen G. Osborne[3], Carl-Johan Rubin[1], Peter R. Grant[4], B. Rosemary Grant[4], Leif Andersson[1,5,6*]

Affiliations:
[1]Department of Medical Biochemistry and Microbiology, Uppsala University, SE-751 23 Uppsala, Sweden.
[2]Department of Life Sciences, Imperial College London, Silwood Park Campus, SL5 7PY Ascot, UK.
[3]School of Natural Sciences, Bangor University, Environment Centre Wales, Deiniol Road, Bangor, LL57 2UW, UK.
[4]Department of Ecology and Evolutionary Biology, Princeton University, Princeton, New Jersey 08544, USA.
[5]Department of Animal Breeding and Genetics, Swedish University of Agricultural Sciences, SE- 75007 Uppsala, Sweden.
[6]Department of Veterinary Integrative Biosciences, Texas A&M University, College Station, Texas 77843-4458, USA.

*Correspondence to: Erik D. Enbody (erik.enbody@gmail.com) and Leif Andersson (leif.andersson@imbim.uu.se)

Lead contact: Erik D. Enbody (erik.enbody@gmail.com)

Summary

Carotenoid-based polymorphisms are widespread in populations of birds, fish, and reptiles[1], but generally little is known about the factors affecting their maintenance in populations[2]. We report a combined field and molecular-genetic investigation of a nestling beak color polymorphism in Darwin's finches. Beaks are pink or yellow, and yellow is recessive[3]. Here we show that the polymorphism arose in the Galápagos half a million years ago through a mutation associated with regulatory change in the *BCO2* gene, and is shared by 14 descendant species. The polymorphism is probably a balanced polymorphism, maintained by ecological selection associated with survival and diet. In cactus finches the frequency of the yellow genotype is correlated with cactus fruit abundance and greater hatching success, and may be altered by introgressive hybridization. Polymorphisms that are hidden as adults, as here, may be far more common than is currently recognized, and contribute to diversification in ways that are yet to be discovered.

Results and Discussion

Adaptive radiations are groups of related organisms that have diversified relatively rapidly from a common ancestor[4,5]. A striking feature of some radiations is that polymorphic variation within species is shared among related species (reviewed in[2]). This observation raises the question: how does variation persist in multiple related species[2,6–8]? Shared polymorphisms originate through shared ancestral variation, repeated mutation and/or introgression, and are maintained by negative frequency-dependent selection, heterozygous advantage or spatiotemporal fluctuations in selective pressures[2,7,8]. Distinguishing among these alternatives requires an understanding of the genetic basis of phenotypic variation, phylogenetic history, and fitness variation in natural populations. This has been rarely achieved, partly because polymorphisms are often associated with large genomic regions containing many genes of uncertain functional importance (e.g.[9–14]), and partly because of the difficulties of determining fitness in nature. Here we report a shared color polymorphism in the radiation of Darwin's finches (Thraupidae) on the Galápagos and Cocos islands. We identify its genetic basis and phylogenetic origin, and take advantage of uniquely banded individuals on one island to consider how ecological factors might contribute to the maintenance of the polymorphism.

Identification of the gene responsible for a nestling color polymorphism

A beak color polymorphism in nestlings has been documented in ten species of Darwin's finches (three *Camarhynchus* and seven *Geospiza*[15]). The beaks of nestlings are either pink or yellow (Figure 1A), recognizable at hatching, and similar in appearance among species. The yellow morphs are otherwise indistinguishable. Pedigrees on Daphne Major Island[3] and Genovesa[16] show that the yellow phenotype is recessively inherited and pink and yellow morphs occur in the

same nest, but the causal gene is unknown. The pink beaks appear pink because the blood supply can be seen. Increasing melanin deposition in the beak obscures phenotypic expression several weeks after fledging and culminates in complete melanization in breeding birds.

In order to identify loci associated with the polymorphism, we focused on two species present on Daphne Major that differ in morph frequencies[3]: *Geospiza scandens* (yellow frequency = ~30%) and *G. fortis* (yellow frequency = ~20%). We sequenced whole genomes at low coverage of 456 individuals of known phenotype (mean depth = 2.2 ± 1.0X) to search for the genetic basis of the polymorphism. We generated genotype likelihoods using the software ANGSD[17] and conducted an association analysis under a generalized logistic regression model that incorporates genotype uncertainty[18] for *G. scandens* (n_{pink} = 98, n_{yellow} = 98) and *G. fortis* (n_{pink} = 130, n_{yellow} = 130) separately with nestling beak color as the response variable. We discovered a small region on chromosome 24 harboring a region strongly associated with the yellow phenotype overlapping the carotenoid-cleaving beta-carotene oxygenase 2 gene (*BCO2*, Figure 1B). Mutations downregulating BCO2 expression or activity are known to increase deposition of carotenoids and pigmented phenotypes in birds, mammals, and reptiles[19–26]. By closely inspecting this region in a combined sample of all 456 finches of the two species we identified a single exonic single nucleotide polymorphism (SNP) with a likelihood ratio test statistic (LRT) exceeding 166 (Figure 1C). It is also the only consistently elevated SNP in an analysis of each species alone (Figure S1), is the best fit variant under a recessive model (see note S1), and occurs on multiple haplotypes (Figure S1C). This SNP (chr24:6,166,878; p6166878 hereafter) leads to a synonymous change 32bp into exon 4 of *BCO2*. We used high coverage sequencing data for 16 pink and 8 yellow individuals (Figure S1D), and a larger subset of individuals of unknown phenotype (Figure S1E), to search for SNPs or structural variants

linked to p6166878 in the vicinity but found none and confirmed the strong phenotype association with p6166878.

In order to further confirm the association for p6166878 we designed a TaqMan SNP assay to genotype 1,631 individuals of known phenotype (Table S1) of five species from two Galápagos islands collected during the period 1975-2012. Ninety-eight percent of observed genotypes matched the genotype predicted from phenotype (Figure 1E). The few mismatched pink phenotypes with yellow genotypes could be the result of mis-phenotyping or limited nutrition[27], but mismatched individuals were notably often clustered in families (Figure S2B, but not by species Figure S2A), suggesting a possible unknown genetic or shared environmental contribution. None of the homozygous pink genotypes exhibited the yellow phenotype.

Origin of the polymorphism

The yellow allele was not found in warbler finches (*Certhidea olivac*ea and *C. fusca*) or in the vegetarian finch (*Platyspiza crassirostris*) with a combined sample size of 42 individuals (Figure 2), and therefore it probably arose by mutation soon after the split between the vegetarian finch lineage and the ground/tree finch lineage roughly half a million years ago (Figure 2). The polymorphism was retained throughout the radiation except in *G. septentrionalis*. All individuals of this species have yellow beaks but, uniquely, they also have yellow legs and yellow skin, and all three features are retained into adulthood[15], strongly suggesting a different genetic basis than for the nestling beak color polymorphism in the other species. We were not able to dissect the genetic basis for yellow color in *G. septentrionalis* because there is no phenotypic variation within this species.

Functional considerations

The functional importance of the observed synonymous change is uncertain, and the presence of an unidentified linked causal variant cannot be completely ruled out (see Conclusions). However, a functional explanation is possible because codon usage can be under strong selection[28] and may have functional consequences on translation[28], RNA stability[29] and transcription[30]. Notably, p6166878 changes the highest frequency valine codon (f_{GTG} = 27.3%) to the lowest (f_{GTA} = 7.6%) in the reference genome. This is in line with the observed phenotypic effect of the yellow mutation, because a lower abundance codon is expected to be associated with lower protein expression[31]. In this case, less BCO2 activity results in more carotenoid deposition in the yellow morph. In fact, we found that yellow homozygotes showed significantly lower *BCO2* expression compared to pink homozygotes in the upper beak of developing embryos (Figure 1F) that were sourced from a variety of different species and islands (Table S1): small sample sizes prohibit species-specific analysis. Among the six heterozygous individuals, the pink allele was expressed more than the yellow allele in five samples tested using a droplet-digital PCR (Figure S2C). Differences in expression between the two alleles, and in the absence of alternative splice variants (Methods), raises the possibility that the synonymous change alters transcription factor binding affinity in exon 4. Further research into tissue-specific expression and the specific transcription factors that regulate *BCO2* is warranted.

Long-term maintenance of the polymorphism

Nucleotide polymorphisms across the genome that are shared among 14 or more species of Darwin's finches make up roughly 5% of all polymorphic sites (Figure S2D). Thus, the *BCO2*

polymorphism lies in the tail of the distribution of polymorphic sites that show extensive multi-species polymorphism in the phylogeny. Such long-term persistence of a polymorphism (Figure 2) implies some form of balancing selection (reviewed in[2,8]). We next consider possible factors that contribute to a balance in the short term.

Heterozygotes might survive better than homozygotes in their first year, but we found no evidence of heterozygote advantage from the last week in the nest to the year after hatching for individuals captured during nest monitoring between 1978-1998 (*G. fortis*: $\chi^2 = 1.2$, $P = 0.5$, df = 2, $n = 964$ nestlings; *G. scandens*: $\chi^2 = 0.2$, $P = 0.9$, df = 2; $n = 326$ nestlings). Since color polymorphisms in birds are well-known to have signaling functions associated with disassortative mating[32], predator avoidance[33], and reproductive parameters[34], among other factors[35], the nestling color variation could have a signaling role, allowing parents to feed offspring preferentially[36]. However, a signaling role was rejected in a previous study because observations made during half-hour nest watches, and parental feeding of recently fledged juveniles, gave no indication of preferential feeding[15].

Alternatively, the significance of the polymorphism might reside in nutritional factors. All species of Darwin's finches obtain carotenoids by feeding on pollen and/or herbivorous insects, mainly Lepidoptera larvae, which parents feed to their nestlings. *G. scandens*, the species on Daphne Major with the highest frequency of the yellow allele, is a specialist feeder on carotenoid-rich pollen from *Opuntia* cactus (Figure 3A, [37]) capable of feeding nestlings almost entirely on a diet of cactus pollen and nectar. In 9 out of 13 years, yellow morph *G. scandens* experienced higher first-year survival than pink morph *G. scandens* (Figure S3), reflected in overall higher survival of the yellow morph (34% vs 29%, , $\chi^2 = 4.31$, $n = 2065$, $P = 0.04$,

Pearson's Chi-squared). Strong differences between some years are consistent with fluctuating selection, in addition to random changes (see note S2), but we did not observe negatively covarying trends expected under frequency-dependent selection. Individuals with the yellow genotype survived conspicuously poorly in 1998, a year with el Niño conditions of abundant rain, repeated breeding, but almost zero cactus flower and fruit production (Figure 3B), whereas in 1991, a similar el Niño year[38] except for plentiful cactus production, the yellow genotype survived better than pink homozygous *G/G* or heterozygous *G/A* individuals. (Figure 4A, Table S2, Generalized linear model: interaction genotype*year, OR = 0.19, 95% CI = 0.04 – 0.82, P = 0.03, n = 183 nestlings). As a consequence, the frequency of the yellow genotype *G. scandens* plummeted with continued high mortality of *G. scandens* and low cactus fruit abundance into the drought of 1999 (Figure 3C).

Although the beak color polymorphism is likely to be balanced, it is not fixed and static. As previously described[39–42], *G. scandens* hybridized occasionally with *G. fortis* and without apparent loss of fitness over a 40-year period. Autosomal genes (alleles) flowed mainly from *G. fortis* to *G. scandens*[39,41] and they included *BCO2* alleles that are more frequently pink in *G. fortis* than in *G. scandens*. We evaluated the introgression of pink alleles using whole-genome analysis of 176 individuals homozygous for the pink allele hatched early or late in the study period. Genome-wide divergence prior to 1995 was higher (F_{ST} = 0.15, n = 88) than after 2008 (F_{ST} = 0.08, n = 88), similar to previous estimates[39]. Four diagnostic *G. fortis* alleles at SNPs in the near vicinity of p6166878 (within 5-kb), rose in frequency by 8-29% in the *G. scandens* population during this time period (Note S2, Table S4). This is consistent with the convergence in yellow allele frequency shown in Figure 3C, which is possibly a consequence of gene flow of *G. fortis*-derived pink alleles into the *G. scandens* population.

Since carotenoids have an essential role in Vitamin A metabolism[43] and in color vision[44], altered *BCO2* expression and carotenoid sequestration may be biochemically advantageous at high intake levels for three reasons. First, deposition in the beak may avoid a toxic accumulation of metabolic breakdown products of circulating carotenoids[43], so that sequestered carotenoids can be metabolized later at a time of lower intake[45]. For example, it is known that excess carotenoid accumulation impairs muscle function in other bird species[46]. Second, the yellow polymorphism could influence maternal investment. Fallahshahroudi et al.[47] found that chicken mothers homozygous for the yellow skin allele, a *BCO2* allele silenced in skin tissue[19], invest more carotenoids in egg yolk than other genotypes[47]. Consistent with this, *G. scandens* mothers with the yellow genotype hatched eggs more successfully than heterozygous individuals (97% vs. 78%: Linear mixed effect model with year-hatched as a random effect, $\chi^2 = 12.1$, $P < 0.001$, df = 2; $n = 138$ nests; Figure 4B, Table S2). The pattern was repeated at different times and in different age groups in the extended breeding season of 1983 (Table S3). Third, reduced *BCO2* expression and carotenoid accumulation may alter spectral tuning in the avian retina, where *BCO2* is required for the biosynthesis of galloxanthin, a key apocarotenoid involved in short-wavelength vision[44]. In the absence of experimental data, visual perception differences among morphs remains unexplored.

Conclusions

The genetic basis of polymorphic traits in natural populations, and selection pressures acting on them, are generally not known[2], although there are a few outstanding exceptions involving supergenes[9–14]. Here we have shown that variation at a single locus (*BCO2*) is responsible for a beak color polymorphism in Darwin's finches. This synonymous mutation associated with the

yellow morph has an uncertain functional consequence, but it changes the highest frequency valine codon to the least abundant in the finch genome, and it is associated with reduced *BCO2* expression. We cannot completely exclude the possibility that this synonymous mutation may be linked to one or several unidentified causal variants. However, it occurs on multiple haplotypes (Figure S1C) and a careful analysis of our genome data did not reveal any other candidate mutation or any haplotype pattern consistent with the presence of two independent causal mutations (both associated with the synonymous variant). Identification of a sequence variant linked to the phenotypic polymorphism has enabled us to trace its origin through phylogenetic analysis to a single mutation occurring in the Galápagos archipelago approximately half a million years ago. The polymorphism has been retained in all descendant species except one. The most parsimonious explanation for its occurrence in many species is that the polymorphism is a shared ancestral condition. Persistence across the radiation is notable because the rarer morph may be lost through drift in the founding of new populations by a limited number of individuals during speciation[2,6]. Nonetheless, Darwin's finches satisfy two conditions that are conducive to retention: high speciation rate[48] and presence of several coexisting, and occasionally interbreeding, closely related species[3,16,49]. Loss through drift is likely to be counteracted by reintroduction through introgression[20,50], especially in the early stages of speciation.

Although we do not fully understand the salient selection pressures, we have identified diet as an important factor, because frequencies of the yellow allele in *G. scandens* are associated with changing diet availability in a cactus specialist. In this species, the frequency of the yellow allele decreased abruptly following a resource-induced crash, which may indicate that any advantage to the yellow allele is lost during prolonged periods of high stress lasting for one or more years. The yellow genotype is relatively common in cactus-specialist species feeding on

carotenoid-rich pollen and tend to survive better in some years when cactus products are plentiful. The selective advantage of the yellow morph under certain environmental conditions must be counterbalanced by a yet unknown selective advantage for the pink morph under other conditions. A contributing factor may be selection that maintains the essential role of BCO2 in spectral tuning[44] or in carotenoid degradation and detoxification[51,52]. However, BCO2 expression may be normal in the liver of the yellow morph, as in the chicken BCO2 mutation[19], meaning the yellow morph does not become toxified. We found evidence of higher hatching success of eggs produced by females of *G. scandens* with the homozygous yellow genotype. This raises the intriguing possibility that these females deposit more carotenoids in egg yolks than other genotypes, an important factor for egg quality in birds[47,53,54], which may influence hatching probability. Together, our results suggest that most of the time the yellow polymorphism is approximately neutral, with morph frequencies occasionally perturbed by introgressive hybridization and episodic fluctuations in selection. For other species carrying the yellow allele at high frequency, such as the *Camarhynchus* tree finches, the frequency of the yellow allele has not been studied, but diet may play a role, because all species uptake carotenoids from flowers or caterpillars[55].

Intraspecies color polymorphisms are exceedingly rare in birds (<3.5% of all birds[35]). Most color polymorphisms that have been studied to date are visible in adults and have signaling functions in contexts of mate choice[11], social dominance[56], camouflage[7] or protective mimicry[57]. The yellow beak polymorphism in Darwin's finches differs from all of these, and is more akin to polymorphisms in Major Histocompatibility Complex (MHC) antigens[50], where fitness advantages are physiological and biochemical. Our study also contributes to recent advances in understanding the genetic basis of carotenoid-based traits[58–65] and a growing appreciation for the

237 role of *BCO2* in carotenoid-based phenotypes in birds[19,22–26], primarily in plumage, suggesting a
238 common role for mediating yellow carotenoid-based traits. Since they are largely or entirely out
239 of sight in adults, literally, such polymorphisms may be far more common than is currently
240 recognized, and contribute to diversification in many ways that are yet to be discovered.

Acknowledgments: The National Genomics Infrastructure (NGI)/Uppsala Genome Center provided service in massive parallel sequencing and the computational infrastructure was provided by the Swedish National Infrastructure for Computing (SNIC) at UPPMAX partially funded by the Swedish Research Council through grant agreement no. 2018-05973. We thank A. Sendell-Price and M. Carneiro for insightful discussion. **Funding:** NSF (USA) funded the collection of material under permits from the Galápagos and Costa Rica National Parks Services and the Charles Darwin Research Station, and in accordance with protocols of Princeton University's Animal Welfare Committee. The study was supported by The Knut and Alice Wallenberg Foundation and Vetenskapsrådet.

Author contributions: LA, PRG, BRG, and EDE conceived and designed the study. PRG and BRG collected blood samples and field observations. EDE conducted all bioinformatic and ecological analyses with input from PRG and BRG. CGS was responsible for all genomic material preparation, sequencing, and pedigree analysis. CGS and HB conducted genotyping. MD, OO, and AA collected samples and generated expression data. CJR generated the genome assembly. EDE wrote the first draft of the manuscript with input from LA, PRG, and BRG and all authors commented on the final manuscript. All authors approved the manuscript before submission.

Declaration of interests: Authors declare no competing interests.

Figure Legends

Figure 1: **Genetic basis for a beak polymorphism in Darwin's finches.**
(A) *G. magnirostris* nestlings with the yellow beak phenotype (left) or pink beak phenotype (right). Images by P.R. Grant. **(B)** Association test result for nestling beak color showing the likelihood ratio test (LRT) statistic per-site genome-wide. The top plot shows *G. fortis* (n_{pink} = 130, n_{yellow} = 130) and bottom *G. scandens* (n_{pink} = 98, n_{yellow} = 98). **(C)** SNP association test results for *G. scandens* and *G. fortis* combined showing the region of strong association on chr24. An exonic SNP in *BCO2* is highlighted (LRT = 166.6). **(D)** Alignment of the first 68bp in exon 4 of *BCO2* from the yellow and pink allele, with amino acids indicated between alignments. The high LRT SNP from **(C)** is highlighted. **(E)** Phenotype to genotype matching using 1,631 individuals of known phenotype. Sample sizes for each group are marked above bars and per-species summaries are shown in Figure S2A. **(F)** Fragments Per Kilobase per Million mapped reads (FPKM) of *BCO2* embryos of several finch species (Table S1), contrasted across known genotypes (n = 35; AA = 3, GA = 6, GG = 26). *P*-values for Tukey's post-hoc analysis is noted above each individual comparison and boxplot hinges correspond to the first and third quantiles, center line is median, and whiskers mark 1.5x the interquartile range. Raw data are shown as points and jittered. See also Figure S1 and Figure S2.

Figure 2: Frequency of the yellow allele across the Darwin's finch radiation.
Left, a species chronogram for Darwin's finches (reproduced from[66]), colored by genera, with the parsimonious origin of the yellow allele marked with a yellow star (previously dated at 546 KYA[48]). A yellow asterisk marks all species where the yellow nestling phenotype has been observed, a black asterisk indicates that the yellow nestling phenotype has not been observed, and no asterisk indicates that the nestling phenotype has not yet been studied in that species. *G. septentrionalis* has a different yellow phenotype (see text). Right, the frequency of the yellow allele (*BCO2* SNP p6166878, allele A) in all finch species with the number of individuals genotyped marked along the vertical axis (including samples from[48,66]). See also Figure S2D.

Figure 3: **Changes in yellow genotype frequency over time in relation to cactus abundance in two Darwin's finch species on Daphne Major.**
(A) Proportion of adult diet during early breeding in *G. scandens* and *G. fortis* (reproduced from[37]). **(B)** Annual maximum *Opuntia* cactus representing fruit availability on Daphne Major. No data were collected in 2005. **(C)** Frequency of the yellow (*A/A*) genotype over 26 years for *G. fortis* (blue) and *G. scandens* (red); points are scaled by sample size. Frequencies are plotted beginning in 1987, one year before blood sampling began. See also Figure S3A and Figure S4.

Figure 4: **Survival and hatching success in relation to genotype in *G. scandens*, the common cactus finch.**
(A) Differences in survival to 1-year after hatching between the 1991 cohort and 1998 cohort. Yellow genotype individuals survived better in 1991 than 1998, corresponding to years of high and low cactus production, respectively. **(B)** Lifetime hatching success for 22 mothers and 138 nests, colored by genotype. Yellow genotype mothers experienced greater hatching success than heterozygotes. We cannot evaluate homozygous pink hatching success, for which we have only

two mothers. 95% confidence intervals are shown and only comparisons with significance $P <$ 0.05 are marked (see summaries in Table S2). See also Figure S3.

STAR METHODS

RESOURCE AVAILABILITY

Further information and requests for resources and reagents should be directed to and will be fulfilled by the lead contacts, Erik D. Enbody (erik.enbody@gmail.com) and Leif Andersson (leif.andersson@imbim.uu.se).

Materials availability

This study did not generate new unique reagents.

Data and code availability

Resequencing data is deposited at NCBI# PRJNA678752. The genome assembly for Camarhynchus_parvulus_V1.1 can be found at NCBI# GCA_902806625.1. Data tables for TaqMan genotypes, list of samples used for whole-genome resequencing, RNAseq sample metadata, and code for bioinformatic analyses are uploaded to the GitHub page of EDE during review, and will be archived at time of publication: (https://github.com/erikenbody/Finch_beak_color_polymorphism).

METHODS DETAILS

Sample collection

Blood was collected as part of a long-term monitoring of finches on Daphne Major and other islands beginning with samples first collected in 1988. Sampling was conducted in accordance with protocols of Princeton University's Animal Welfare Committee, and stored on EDTA-soaked filter paper in Drierite to preserve red blood cells for DNA extraction later. Additional details on sample collection can be found elsewhere[3], as well as for samples collected on other islands and used in the TaqMan assays[48,66]. Nestlings were phenotyped for the beak color polymorphism by eye and scored for the presence or absence of having extensive yellow on the lower mandible. Although individual phenotypes change with age (the beak is eventually covered by melanin), the beak color of nestlings is dichotomous in variation and binned visually for the presence or absence of yellow. Among Daphne individuals, we selected all 98 *G. scandens* and all 130 *G. fortis* carrying the yellow phenotype for which we have collected genetic material for. We then selected an equal number of pink individuals per species (pink is the more common phenotype, so there are more samples collected of the pink phenotype), for a total of 456 samples used for low-coverage sequencing and genome-wide association analysis. Later, we sequenced an additional 151 pink individuals to test for introgression (see section on introgression below). This study includes in total 607 Darwin's finch whole-genome samples sequenced at low coverage. Embryos (n = 35, Table S1) were collected on Santa Cruz and Pinta according to[67]. Tissues were stored in RNAlater (ThermoFisher, CA) until further use.

DNA extraction library preparation

We extracted DNA from blood on filter paper using a custom salt preparation protocol. Briefly, we submerged clipped blood on filter paper in a buffer containing 400mM NaCl, 2mM EDTA (pH 8.0), 10mM TrisHCl (pH 8.0), and dH20. Next, we added a freshly prepared buffer

containing 5% SDS, proteinase K (2mg/mL), and dH20. Samples were incubated overnight at 55°C, the filter paper removed, and 135µL of saturated NaCl was added to the mixture. The sample tube was vortexed and spun down at 4,000 rpm for 15min at 4°C and the supernatant transferred to a new 2mL tube. DNA was precipitated using 2 volumes 95% EtOH and mixed by inverting the tube. Finally, samples were spun at 13.3rpm for 3min to pellet the DNA, EtOH removed, and 50-200uL TE added to elute the DNA. DNA concentration was measured on a Nanodrop (ThermoFisher, CA).

We generated fragment libraries for whole-genome sequencing using a custom Tn5-based tagmentation protocol based on[68]. Briefly, we assembled the Tn5 transposon construct using the stock Tn5 (prepared by Karolinska Institutet Protein Science Facility) and primers described in[68]:

Tn5MErev: 5;-[phos]CTG TCTCTTATACACATCT-3'

Tn5ME-A (Illumina FC-121-1030): 5'-TCGTCGGCAGCGTCAGATGTGTATAAGAGACAG-3'

Tn5ME- B (Illumina FC-121-1031): 5'-GTCTCGTGGGCTCGGAGATGTGTA TAAGAGACAG-3'

Samples were tagmented by adding to a solution containing the Tn5 construct and H_20, 5x TAPs, and 40% PEG. The mixture was incubated on a Bio-Rad thermocycler (Bio-Rad, CA) for 10min at 55°C. Next, genomic libraries were PCR enriched using Kapa Biosystems HiFi HotStart (Wilmington, MA) PCR kit (annealing temperature 63°C). DNA libraries were size selected using .38X and .16X Ampure XP beads (Brea, CA) for a target insert size of 350bp, and resulting product quantified on a Tecan microplate reader (Tecan Life Sciences, Switzerland) using Qubit (ThermoFisher, CA) reagents. Samples were pooled in equimolar concentrations and a final size selection performed using .45X and .3X Ampure beads on the resulting pool. Pools were sequenced on an Illumina NovaSeq S4 flow cell (Illumina, CA) with a target sequencing depth of 2x.

TaqMan genotyping assay

Custom SNP genotyping TaqMan assay (ThermoFisher, CA) were applied to perform genotypic analysis of the SNP of interest in exon 4 of *BCO2*. We designed primers (BCO2_F: 5'-TGTTTCAGAACCCAGTGACAACT-3'; BCO2_R:5'-TTCCAGTGTCTCTGGGTCCA-3') and probes (BCO2_VIC:5'-ATGTGAACTACGTGCTGTAC-3'; BCO2_FAM:5'-ATGTGAACTACGTACTGTAC-3') for the SNP of interest on chr24:6166878 (A/G). We used this assay to genotype 2,859 individuals, for which 1,631 had a known nestling beak phenotype.

RNA sample preparation and sequencing

We dissected the upper beak primordia of 35 Darwin's finch embryos (6 *Geospiza magnirostris*, 7 *G. fortis*, 7 *G. fuliginosa*, 8 *Camarhynchus psittacula*, 1 *C. parvulus*, and 6 *Platyspiza crassirostris*) and extracted RNA with E.Z.N.A. Total RNA Kit I (Omega Bio-tek, GA). We prepared cDNA libraries with the NEBNext Ultra RNA Library Prep Kit for Illumina (NewEngland Biolabs, MA) with poly(A) selection. The libraries were then sequenced on HiSeq 4000 (Illumina, CA).

In order to search for splice variations, RT-PCR was applied to amplify the regions around p6166878 in cDNA by the use of forward 5'- CCCATCCCAGCCAAGATCAA-3' and reverse

5'- CGTAGTGGGGATGAGCTGTG-3' primers under the following conditions: 95°C for 5 min, followed by 35 cycles of 95°C for 30 s, 60°C for 30 s and 72°C for 1 min. The amplified fragments were subjected to Sanger sequencing where splice variants were searched for by eye and none were detected.

ddPCR for allele specific expression in heterozygotes

Droplet digital PCR was performed using Bio-Rad QX100 Droplet Digital PCR system (Bio-Rad, CA) to analyze allele-specific RNA expression. The reaction mix was prepared by using 11 µl of 2X ddPCR Supermix for Probes (no dUTP)(Bio-Rad, CA), 1.1 µl 20× Primer and Probe Mix (final concentration of 800 and 300nM, respectively), 7.9 µl Nuclease free water, and 2 µl reverse transcriptase product. Probes were reused from the TaqMan analysis described above and primers crossing exon-intron junctions are listed below. Twenty microliters of the prepared mixture were loaded into a disposable droplet generator cartridge (Bio-Rad, CA), along with 70 µL of droplet generation oil for probe (Bio-Rad, CA) to generate droplet with the QX100 droplet generator (Bio-Rad, CA). After generation, samples were transferred to a 96-well plate and cycled in a C1000 touch Thermal Cycler (Bio-Rad, CA) under the following cycling protocol: 95°C for 10min, then 42 cycles of 95°C for 30s (denaturation) and 58°C for 120s (annealing), followed by post-cycling steps of 98°C for 10min and an infinite 10°C hold. The ramp rate among the steps of the amplification was adjusted to 1°C/sec. The cycled plate was then read in the QX100 Droplet Reader (Bio-Rad. CA) and the data was analyzed with QuantaSoft software (Bio-Rad, CA). Primers:

BCO2_F2 - GCCACAACCCAGTGACAACT
BCO2_R1 - TTCCAGTGTCTCTGGGTCCA

QUANTIFICATION AND STATISTICAL ANALYSIS

Population genomics

All Illumina short reads were mapped to the chromosome-scale Camarhynchus_parvulus_V1.1 genome assembly (GCA_902806625.1) using BWA mem v0.7.17[69] and the resulting BAMs were sorted using SAMTOOLS v1.10 (http://www.htslib.org/). Sequencing coverage was estimated for chromosome 4 (a large, representative subset) using the SAMTOOLS coverage command. We used ANGSD v0.935-33-g79d9455 (Analysis of Next Generation Sequencing Data[17]) to estimate genotype likelihoods used for running association tests. We ran the following commands for each species (*G. scandens* and *G. fortis*; n = 2 runs total), which outputs a beagle file of genotype likelihoods:

```
$ANGSD_PATH/angsd -b $BAMLIST1 -ref $REFGENOME -anc $REFGENOME -r $INTERVAL \
              -out Results_gwas/${POP1}_${POP2}_${INTERVAL}.ref \
              -uniqueOnly 1 -remove_bads 1 -only_proper_pairs 0 -trim 0 \
              -minMapQ 20 -minQ 20 -doCounts 1 \
              -domajorminor 1 -domaf 1 \
              -GL 1 -P 5 -doGlf 2 -SNP_pval 1e-6 -minMaf 0.05 \
              -dumpCounts 1
```

We next generated an estimate of relatedness by calculating principal components using all sites on the chromosome being run using PCAngsd v1.01[70], and processed output using a custom R script:

```
python $PCANGSD/pcangsd/pcangsd.py -beagle
Results_gwas/${POP1}_${POP2}_${INTERVAL}.ref.beagle.gz -o
Results_gwas/${POP1}_${POP2}_${INTERVAL}.ref.pcangsd -threads 5

Rscript ~/bc/gwas_angsd/get_PCs.R
Results_gwas/${POP1}_${POP2}_${INTERVAL}.ref.pcangsd.cov
```

The first two principal components were used as an estimate of relatedness to run the following association test in ANGSD, which performs the logistic regression score test described in[18] under a recessive model with pink coded as 0 and yellow coded as 1:

```
$ANGSD_PATH/angsd -doMaf 4 \
-beagle Results_gwas/${POP1}_${POP2}_${INTERVAL}.ref.beagle.gz \
-fai $FAIFILE  -yBin scandens_bin_pheno.txt -doAsso 2 -model recessive -cov
Results_gwas/${POP1}_${POP2}_${INTERVAL}.ref.PC1_PC2.txt \
-out Results_gwas/${POP1}_${POP2}_${INTERVAL}.ref.lrt.2.rec
```

We extracted allele frequencies at each site used in the association test on chromosome 24 (n = 111,890) by running ANGSD for *G. fortis* yellow, *G. fortis* pink, *G. scandens* yellow, and *G. scandens* pink (n = 4 runs) with the following settings:

```
$ANGSD_PATH/angsd -b $BAMLIST1 -ref $REFGENOME -anc $ANCESTRAL \
              -r $INTERVAL -sites $SITES \
              -out Results_af/${POP1}_${INTERVAL}_BALANCED.all_sites \
              -uniqueOnly 1 -remove_bads 1 -only_proper_pairs 0 -trim 0 \
              -minMapQ 20 -minQ 20 -doCounts 1 \
              -domajorminor 5 -domaf 2 \
              -GL 1 -P 5 -SNP_pval 1e-6
```

All subsequent analysis of association test results were performed using custom scripts in R v4.0.3[71] and various Tidyverse packages[72].

We created a neighbor-joining tree using PCAngsd v1.01[70] for all homozygous AA (n = 176) and GG individuals (n = 80) for the region 5-kb up and downstream of the p6166878 variant using a beagle file generated as described above for the association analysis. PCAngsd generates neighbor-joining trees based on a covariance matrix of individual allele frequencies.

Bioinformatic analysis of introgression

After the identification of the *BCO2* variant of interest at p6166878, we selected an additional 151 individuals to sequence at low-coverage whole-genome sequencing (mean depth = 1.9 ± 1.2X) to test the hypothesis that the frequency of the pink allele changes in the *G. scandens* population due to introgressive hybridization with *G. fortis.* We selected all the *G. scandens* samples homozygous for the pink allele and were hatched after the year 2008 as representative of samples collected "late" in the study (n =44). We next randomly selected an equal number of *G. fortis* samples that were homozygous for the pink allele and were hatched after the year 2008 (n = 44). In order compare samples to those collected early in the study, we sequenced an equal number of randomly selected samples hatched between 1988 and 1995 for *G. fortis* (n = 44) and *G. scandens* (n = 44), all homozygous for the pink allele. 25 of these samples were already

sequenced for the genome-wide association study described earlier (i.e. 176 samples were used in this analysis, 151 of them uniquely generated for introgression analysis). We only selected homozygous pink alleles in order to evaluate if the frequency of the pink allele in the *G. scandens* population rose in frequency as a consequence of introgression from *G. scandens*.

We used ANGSD v0.935-33-g79d9455 to generate allele frequency estimates for each of the four groups (early *G. fortis*, early *G. scandens*, late *G. fortis*, late *G. scandens*) separately.

```
$ANGSD_PATH/angsd -b $BAMLIST1 -ref $REFGENOME -anc $REFGENOME -r $INTERVAL \
              -out Results_fortis_scandens/${POP1}_${INTERVAL}.ref \
              -uniqueOnly 1 -remove_bads 1 -only_proper_pairs 0 -trim 0 \
              -minMapQ 20 -minQ 20 -doCounts 1 \
              -GL 1 -P 8 \
              -doSaf 1
```

We next used the realSFS command in ANGSD to generate the 2d SFS (site frequency spectrum) which was used as input to the realSFS `fst index` command to calculate pairwise genomic divergence (i.e. F_{ST}) between the two species at both the early and late time points. F_{ST} was then summarized in 10,000-kb, non-overlapping, windows using the realSFS `fst stats2` command. We calculated mean genome-wide F_{ST} between *G. fortis* and *G. scandens* at both the early (pre-1995) and late (post-2008) time periods using these windowed-values. Per-site F_{ST} values were extracted for the region 5-kb upstream and downstream (Table S4) using the realSFS `fst print` command. We identified five SNPs exceeding the 99.95% percentile of early F_{ST} values in the vicinity of p6166878 using custom R-scripts. Allele frequencies within each of the four groups were additionally extracted using the `-domajorminor 5 -domaf 2` for the *BCO2* region in order to calculate the change of allele frequency between early and late *G. scandens* samples (Table S4). For this analysis, conducted using custom R-scripts, we set the major allele as the most common allele in early *G. fortis* samples.

Analysis of high coverage data

Short read sequencing data for 293 samples from 20 Darwin's finch species and two outgroup species was accessed from NCBI sequence read archive (www.ncbi.nlm.nih.gov/sra) BioProjects PRJNA392917[66], PRJNA263122[48] and PRJNA301892[73]. Two homozygous yellow (*A/A*) from *G. scandens* and *G. fortis* (n = 4 total) that were sequenced at low coverage were also sequenced to a target coverage of 15x (this study, PRJNA678752). All short-reads were aligned to Camarhynchus_parvulus_V1.1 using BWA mem v0.7.17[69]. SNPs were called using GATK's HaplotypeCaller and joint genotyping using GenotypeGCVFs (v4.1.4.1[74]). Filtering was done for SNPs using filter-expressions in VariantFiltration and only biallelic SNPs were retained:

```
"QUAL < 100 || MQ < 40.0 || MQ > 80.0 || MQRankSum < -4.0 || MQRankSum > 4.0
|| ReadPosRankSum < -4.0 || ReadPosRankSum > 4.0 || QD < 5.0 || FS > 30.0 ||
DP < 50 || DP > 29300"
```

And removing genotypes with low depth and low genotype quality using -G-filter:

```
"DP < 1 || DP > 200 || GQ < 10"
```

We searched for indels and SNPs that might be linked to p6166878 by searching the unfiltered joint-genotyped VCF for all SNPs and indels 200-kb upstream and downstream of p6166878.

We calculated allele frequency for homozygous alternative individuals (*A/A* and *G/G*) at this position and removed variants with a minor allele frequency < 0.05. Delta allele frequency was calculated as the difference in frequency of non-reference allele in individuals genotyped as homozygous yellow or homozygous pink based on SNP p6166878 (Figure S1E).

We extracted genotypes at the SNP position of interest (p6366878) using BCFtools v1.10 (http://www.htslib.org/)**:**

```
bcftools query -r chr24:5966878-6366878 -f '[%GT\t]\n' $VCF > p
6366878_raw.genos
```

We calculated the frequency of the yellow allele (A) by counting the number of alternate alleles per species and dividing by 2n (n = number of individuals per population). Allele frequencies depicted in Figure 2 include a combination of high coverage samples (n = 293) and samples that were individually genotyped (see below, n = 2,859), but we omitted samples that were determined from field observations to be of hybrid origin in Figure 2.

In order to approximate the timing of the appearance of the yellow allele (A), we placed the origin of the polymorphism on an existing Darwin's finch phylogeny. We downloaded a recent phylogenetic hypothesis for all species that used a maximum-likelihood approach on a concatenated SNP matrix to generate a tree ([66], https://treebase.org/treebase-web/search/study/summary.html?id=21803). We pruned this tree to one branch per species and converted the tree to an ultrametric tree using makeChronosCalib to set root time to 1 MYA based on previous estimates[48] with the R package ape[75]. We then converted the original tree to a chronos time tree using the following command:

```
timetree <- chronos(finch.pruned.tre, lambda = 1, model = "correlated",
calibration = mycalibration, control = chronos.control() )
```

The final plot was produced using ggtree for the base tree[76] and adding the bar plots of allele frequency[77]. The estimated divergence time between *P. crassirostris* (lacking the A allele) and all *Geospiza, Camarhynchus,* and *Pinaroloxias* species was estimated using this method as 456 KYA compared to 546±74 reported in a previous analysis[48].

For all species in the dataset that carry the yellow allele (A, n = 15), we tabulated the number of SNPs that are shared between n={1..15} species. Specifically, for each SNP called (n = 26,056,248) in the dataset, we summed the number of species carrying at least 1 alternate allele at that position. Allele frequencies per species were tallied using bcftools, summed using custom bash scripts (allele_sharing.sh), and plotted using custom R scripts (plot_af.R).

Allele specific expression

For 29 individuals for which we have RNAseq data, we also had genomic DNA available. For these individuals we used the same TaqMan assay to determine genotype. For all other individuals we inferred genotype based on RNA sequencing depth. This includes 1 AA, 4 GG, and 1 GA individuals. Before mapping RNAseq data, Illumina adaptor and primer sequences were removed with CutAdapt v.1.9[78] and low-quality bases (PHRED < 20) were removed using Trim Galore (v.0.4.1, available at

http://www.bioinformatics.babraham.ac.uk/projects/trim_galore/) with default settings. Cleaned RNAseq reads were then mapped to the genome and Fragments Per Kilobase of transcript per Million mapped reads (FPKM) was calculated using the HISAT2 (v. 2.1.0) - StringTie (v. 1.3.6) – Ballgown (v. 2.20.0) pipeline[79]. For the 6 individuals we genotyped using RNAseq data, genotypes were called using SAMTOOLS and BCFtools v1. 9:

```
samtools mpileup -Q 20 -q 20 -t DP4,DP -vuf ${ref} *.bam | bcftools call -M -
f GQ -mg 3 -Ov > snps.vcf
```

We compared the number of Fragments Per Kilobase of transcript per Million mapped reads using a three-way ANOVA with the aov command and post-hoc comparisons using the TukeyHSD command in R (v4.0.3).

Codon usage bias

We queried the Codon and Codon Pair Usage Tables (CoCoPUTs[80]) for the reference genome assembly build for Camarhynchus_parvulus_V1.1. The CoCoPUTs tool pulls from the GenBak refseq database to compute codon usage for publically available data. The frequency of the four valine codons in the *C. parvulus* genome are as follows:

GTT = 13.50 %
GTC = 12.61 %
GTA = 7.63 %
GTG = 27.25 %

Cactus fruit abundance

We counted the number of flowers and fruits on 10 marked *Opuntia* bushes at 7 to 10-day intervals during each annual visit to Daphne Major Island. We focus on fruits as a measure of annual food availability because the sample of fruits represents all flowers produced up to that time. For an analysis of survival from hatching to the beginning of the following year we focus on flowers as a source of pollen and nectar at the time that nestlings are fed. Flower numbers for 1991 and 1998 are shown in Figure S3B. Flowering typically begins in October or November. Flowers and fruits were counted in January, February and occasionally later at the end of the flowering season.

Survival analysis and hatching success

We used a 2-sided Pearson's chi-squared test in R (v4.0.3) to test for a difference in first-year survival among genotypes for all *G. scandens* (n = 326) and *G. fortis* (n = 964) nestlings captured with genetic samples during regular nest monitoring that took place between 1978 and 1998. When analyzing survival of the two morphs in *G. scandens* across all years, we used a 2-sided Pearson's chi-squared test with a Yate's continuity correction in R (v4.0.3) to test for differences in morph survival for 2065 nestlings with known phenotypes (see note S3). The difference in sample size between these two approaches is due to the larger number of individuals with phenotypic data than were available for genetic analysis (i.e. not all nestlings had samples for genetic analysis collected).

We modeled first year survival in 1991 and 1998 using a generalized linear model (GLM) in R (v4.0.3) with survival to one year after hatching as a binary response variable. We included

643 *BCO2* genotype, year, and the interaction between the two to test the hypothesis that first year
644 survival differed between 1991 and 1998. We used the tab_model function from sjPlot to
645 summarize models[81] and report odds ratios.
646
647 We analyzed lifetime mean female hatching success in *G. scandens* using linear mixed models in
648 the package lmerTest[82]. Mean hatching rate was calculated per nest as the ratio of number of
649 hatched divided by the total number of eggs laid. Consequently, hatching rate was only tabulated
650 for individuals where the number of eggs laid and hatched were known. We removed nests
651 where no eggs hatched (which could have been the result of other factors, such as nest predation)
652 and birds with only one nest (which prevented a reliable mean rate across nests). One yellow
653 phenotype individual was included as *A/A* who failed to amplify using the TaqMan assay. Each
654 individual was given a single value for lifetime average hatching success, which was used as the
655 response variable in the LMM. We included cohort (year hatched) of each female as a random
656 effect in the model. We used the Anova command (type = "II") from the car package[83] to test
657 significance of predictor effects and tab_model from sjPlot to summarize models[81].

References

1. Gray, S.M., and McKinnon, J.S. (2007). Linking color polymorphism maintenance and speciation. Trends in Ecology and Evolution *22*, 71–79.
2. Jamie, G.A., and Meier, J.I. (2020). The persistence of polymorphisms across species radiations. Trends in Ecology & Evolution *35*, 795–808.
3. Grant, P.R., and Grant, B.R. (2014). 40 years of evolution: Darwin's Finches on Daphne Major Island (Princeton University Press).
4. Schluter, D. (2000). The Ecology of Adaptive Radiation (Oxford University Press).
5. Stroud, J.T., and Losos, J.B. (2016). Ecological opportunity and adaptive radiation. Annual Review of Ecology, Evolution, and Systematics *47*, 507–532.
6. Guerrero, R.F., and Hahn, M.W. (2017). Speciation as a sieve for ancestral polymorphism. Molecular Ecology *26*, 5362–5368.
7. Nosil, P., Villoutreix, R., De Carvalho, C.F., Farkas, T.E., Soria-Carrasco, V., Feder, J.L., Crespi, B.J., and Gompert, Z. (2018). Natural selection and the predictability of evolution in timema stick insects. Science *359*, 765–770.
8. Llaurens, V., Whibley, A., and Joron, M. (2017). Genetic architecture and balancing selection: the life and death of differentiated variants. Molecular Ecology *26*, 2430–2448.
9. Villoutreix, R., De Carvalho, C.F., Soria-Carrasco, V., Lindtke, D., De-La-Mora, M., Muschick, M., Feder, J.L., Parchman, T.L., Gompert, Z., and Nosil, P. (2020). Large-scale mutation in the evolution of a gene complex for cryptic coloration. Science *369*, 460–466.
10. Küpper, C., Stocks, M., Risse, J.E., dos Remedios, N., Farrell, L.L., McRae, S.B., Morgan, T.C., Karlionova, N., Pinchuk, P., Verkuil, Y.I., et al. (2016). A supergene determines highly divergent male reproductive morphs in the ruff. Nature Genetics *48*, 79–83.
11. Lamichhaney, S., Fan, G., Widemo, F., Gunnarsson, U., Thalmann, D.S., Hoeppner, M.P., Kerje, S., Gustafson, U., Shi, C., Zhang, H., et al. (2015). Structural genomic changes underlie alternative reproductive strategies in the ruff (*Philomachus pugnax*). Nature Genetics *48*, 84–88.
12. Nishikawa, H., Iijima, T., Kajitani, R., Yamaguchi, J., Ando, T., Suzuki, Y., Sugano, S., Fujiyama, A., Kosugi, S., Hirakawa, H., et al. (2015). A genetic mechanism for female-limited Batesian mimicry in Papilio butterfly. Nature genetics *47*, 405–9.
13. Toomey, M.B., Marques, C.I., Andrade, P., Araújo, P.M., Sabatino, S., Gazda, M.A., Afonso, S., Lopes, R.J., Corbo, J.C., and Carneiro, M. (2018). A non-coding region near Follistatin controls head colour polymorphism in the Gouldian finch. Proceedings of the Royal Society B: Biological Sciences *285*, 20181788.
14. Kim, K.-W., Jackson, B.C., Zhang, H., Toews, D.P.L., Taylor, S.A., Greig, E.I., Lovette, I.J., Liu, M.M., Davison, A., Griffith, S.C., et al. (2019). Genetics and evidence for balancing selection of a sex-linked colour polymorphism in a songbird. Nature Communications *10*, 1852.
15. Grant, P.R., Boag, P.T., and Schluter, D. (1979). A bill color polymorphism in young Darwin's finches. The Auk *96*, 800–802.
16. Grant, B.R., and Grant, P.R. (1989). Evolutionary Dynamics of a Natural Population: The Large Cactus Finch of the Galapagos (University of Chicago Press).
17. Korneliussen, T.S., Albrechtsen, A., and Nielsen, R. (2014). ANGSD: Analysis of next generation sequencing data. BMC Bioinformatics *15*, 356.
18. Skotte, L., Korneliussen, T.S., and Albrechtsen, A. (2012). Association testing for next-

generation sequencing data using score statistics. Genetic Epidemiology *36*, 430–437.
19. Eriksson, J., Larson, G., Gunnarsson, U., Bed'hom, B., Tixier-Boichard, M., Strömstedt, L., Wright, D., Jungerius, A., Vereijken, A., Randi, E., et al. (2008). Identification of the Yellow Skin Gene Reveals a Hybrid Origin of the Domestic Chicken. PLoS Genetics *4*, e1000010.
20. Andrade, P., Pinho, C., de Lanuza, G.P. i., Afonso, S., Brejcha, J., Rubin, C.J., Wallerman, O., Pereira, P., Sabatino, S.J., Bellati, A., et al. (2019). Regulatory changes in pterin and carotenoid genes underlie balanced color polymorphisms in the wall lizard. Proceedings of the National Academy of Sciences of the United States of America *116*, 5633–5642.
21. Våge, D.I., and Boman, I.A. (2010). A nonsense mutation in the beta-carotene oxygenase 2 (BCO2) gene is tightly associated with accumulation of carotenoids in adipose tissue in sheep (*Ovis aries*). BMC Genetics *11*, 10.
22. Toews, D.P.L., Taylor, S.A., Vallender, R., Brelsford, A., Butcher, B.G., Messer, P.W., and Lovette, I.J. (2016). Plumage genes and little else distinguish the genomes of hybridizing warblers. Current Biology *26*, 2313–2318.
23. Baiz, M.D., Wood, A.W., Brelsford, A., Lovette, I.J., and Toews, D.P.L. (2021). Pigmentation genes show evidence of repeated divergence and multiple bouts of introgression in Setophaga warblers. Current Biology *31*, 643-649.e3.
24. Gazda, M.A., Araújo, P.M., Lopes, R.J., Toomey, M.B., Andrade, P., Afonso, S., Marques, C., Nunes, L., Pereira, P., Trigo, S., et al. (2020). A genetic mechanism for sexual dichromatism in birds. Science *368*, 1270–1274.
25. Gazda, M.A., Toomey, M.B., Araújo, P.M., Lopes, R.J., Afonso, S., Myers, C.A., Serres, K., Kiser, P.D., Hill, G.E., Corbo, J.C., et al. (2020). Genetic basis of de novo appearance of carotenoid ornamentation in bare parts of canaries. Molecular Biology and Evolution *37*, 1317–1328.
26. Walsh, N., Dale, J., McGraw, K.J., Pointer, M. a., and Mundy, N.I. (2012). Candidate genes for carotenoid coloration in vertebrates and their expression profiles in the carotenoid-containing plumage and bill of a wild bird. Proceedings of the Royal Society B *279*, 58–66.
27. Hill, G.E. (2002). A Red Bird in a Brown Bag: The Function and Evolution of Colorful Plumage in the House Finch (Oxford University Press).
28. Machado, H.E., Lawrie, D.S., and Petrov, D.A. (2020). Pervasive strong selection at the level of codon usage bias in *Drosophila melanogaster*. Genetics *214*, 511–528.
29. Carneiro, R.L., Requião, R.D., Rossetto, S., Domitrovic, T., and Palhano, F.L. (2019). Codon stabilization coefficient as a metric to gain insights into mRNA stability and codon bias and their relationships with translation. Nucleic Acids Research *47*, 2216–2228.
30. Zhou, Z., Dang, Y., Zhou, M., Li, L., Yu, C., Fu, J., Chen, S., and Liu, Y. (2016). Codon usage is an important determinant of gene expression levels largely through its effects on transcription. Proceedings of the National Academy of Sciences *113*, E6117–E6125.
31. Gouy, M., and Gautier, C. (1982). Codon usage in bacteria: Correlation with gene expressivity. Nucleic Acids Research *10*, 7055–7074.
32. Tuttle, E.M. (2003). Alternative reproductive strategies in the white-throated sparrow: Behavioral and genetic evidence. Behavioral Ecology *14*, 425–432.
33. Koskenpato, K., Lehikoinen, A., Lindstedt, C., and Karell, P. (2020). Gray plumage color is more cryptic than brown in snowy landscapes in a resident color polymorphic bird.

Ecology and Evolution *10*, 1751–1761.
34. Harris, M.P., Rothery, P., and Wanless, S. (2003). Increase in frequency of the bridled morph of the Common Guillemot Uria aalge on the Isle of May, 1946-2000: A return to former levels? Ibis *145*, 22–29.
35. Roulin, A. (2004). The evolution, maintenance and adaptive function of genetic colour polymorphism in birds. Biological Reviews of the Cambridge Philosophical Society *79*, 815–848.
36. Lyon, B.E., Eadie, J.M., and Hamilton, L.D. (1994). Parental choice selects for ornamental plumage in American coot chicks. Nature *371*, 240–243.
37. Grant, B.R. (1996). Pollen Digestion by Darwin's Finches and Its Importance for Early Breeding. Ecology *77*, 489–499.
38. Grant, P.R., Grant, B.R., Keller, L.F., and Petren, K. (2000). Effects of El Nino events on Darwin's finch productivity. Ecology *81*, 2442–2457.
39. Lamichhaney, S., Han, F., Webster, M.T., Grant, B.R., Grant, P.R., and Andersson, L. (2020). Female-biased gene flow between two species of Darwin's finches. Nature Ecology & Evolution *4*, 979–986.
40. Grant, P.R., and Grant, B.R. (2010). Conspecific versus heterospecific gene exchange between populations of Darwin's finches. Philosophical Transactions of the Royal Society B: Biological Sciences *365*, 1065–1076.
41. Grant, P.R., and Grant, B.R. (2020). Triad hybridization via a conduit species. Proceedings of the National Academy of Sciences of the United States of America *117*, 7888–7896.
42. Grant, P.R., Grant, B.R., Markert, J.A., Keller, L.F., and Petren, K. (2004). Convergent Evolution of Darwin'S Finches Caused By Introgressive Hybridization and Selection. Evolution *58*, 1588–1599.
43. Kiefer, C., Hessel, S., Lampert, J.M., Vogt, K., Lederer, M.O., Breithaupt, D.E., and Von Lintig, J. (2001). Identification and characterization of a mammalian enzyme catalyzing the asymmetric oxidative cleavage of Provitamin A. Journal of Biological Chemistry *276*, 14110–14116.
44. Toomey, M.B., Lind, O., Frederiksen, R., Curley, R.W., Riedl, K.M., Wilby, D., Schwartz, S.J., Witt, C.C., Harrison, E.H., Roberts, N.W., et al. (2016). Complementary shifts in photoreceptor spectral tuning unlock the full adaptive potential of ultraviolet vision in birds. eLife *5*, 1–27.
45. McGraw, K.J., and Toomey, M.B. (2010). Carotenoid accumulation in the tissues of zebra finches: Predictors of integumentary pigmentation and implications for carotenoid allocation strategies. Physiological and Biochemical Zoology *83*, 97–109.
46. Huggins, K.A., Navara, K.J., Mendonça, M.T., and Hill, G.E. (2010). Detrimental effects of carotenoid pigments: the dark side of bright coloration. Naturwissenschaften *97*, 637–644.
47. Fallahshahroudi, A., Sorato, E., Altimiras, J., and Jensen, P. (2019). The Domestic BCO2 Allele Buffers Low-Carotenoid Diets in Chickens: Possible Fitness Increase Through Species Hybridization. Genetics *212*, 1445–1452.
48. Lamichhaney, S., Berglund, J., Almén, M.S., Maqbool, K., Grabherr, M., Martinez-Barrio, A., Promerová, M., Rubin, C.-J., Wang, C., Zamani, N., et al. (2015). Evolution of Darwin's finches and their beaks revealed by genome sequencing. Nature *518*, 371–375.
49. Grant, P.R., Grant, B.R., and Petren, K. (2005). Hybridization in the Recent Past. The

American Naturalist *166*, 56–67.
50. Hedrick, P.W. (2013). Adaptive introgression in animals: Examples and comparison to new mutation and standing variation as sources of adaptive variation. Molecular Ecology *22*, 4606–4618.
51. Amengual, J., Lobo, G.P., Golczak, M., Li, H.N.M., Klimova, T., Hoppel, C.L., Wyss, A., Palczewski, K., and von Lintig, J. (2011). A mitochondrial enzyme degrades carotenoids and protects against oxidative stress. The FASEB Journal *25*, 948–959.
52. Wu, L., Guo, X., Hartson, S.D., Davis, M.A., He, H., Medeiros, D.M., Wang, W., Clarke, S.L., Lucas, E.A., Smith, B.J., et al. (2017). Lack of β, β-carotene-9′, 10′-oxygenase 2 leads to hepatic mitochondrial dysfunction and cellular oxidative stress in mice. Molecular Nutrition & Food Research *61*, 1600576.
53. Koutsos, E.A., Clifford, A.J., Calvert, C.C., and Klasing, K.C. (2003). Maternal carotenoid status modifies the incorporation of dietary carotenoids into immune tissues of growing chickens (Gallus gallus domesticus). Journal of Nutrition *133*, 1132–1138.
54. Surai, P.F., and Speake, B.K. (1998). Distribution of carotenoids from the yolk to the tissues of the chick embryo. Journal of Nutritional Biochemistry *9*, 645–651.
55. Bock, W.J. (1963). Morphological differentiation and adaptation in the Galápagos finches. The Auk *80*, 202–207.
56. Dey, C.J., Valcu, M., Kempenaers, B., and Dale, J. (2015). Carotenoid-based bill coloration functions as a social, not sexual, signal in songbirds (Aves: Passeriformes). Journal of Evolutionary Biology *28*, 250–258.
57. Jay, P., Whibley, A., Frézal, L., Rodríguez de Cara, M.Á., Nowell, R.W., Mallet, J., Dasmahapatra, K.K., and Joron, M. (2018). Supergene evolution yriggered by the introgression of a chromosomal inversion. Current Biology *28*, 1839-1845.e3.
58. Aguillon, S.M., Walsh, J., and Lovette, I.J. (2021). Extensive hybridization reveals multiple coloration genes underlying a complex plumage phenotype. Proceedings of the Royal Society B: Biological Sciences *288*, 20201805.
59. Toomey, M.B., Lopes, R.J., Araújo, P.M., Johnson, J.D., Gazda, M.A., Afonso, S., Mota, P.G., Koch, R.E., Hill, G.E., Corbo, J.C., et al. (2017). High-density lipoprotein receptor SCARB1 is required for carotenoid coloration in birds. Proceedings of the National Academy of Sciences *114*, 5219–5224.
60. Khalil, S., Welklin, J.F., McGraw, K.J., Boersma, J., Schwabl, H., Webster, M.S., and Karubian, J. (2020). Testosterone regulates CYP2J19 -linked carotenoid signal expression in male red-backed fairywrens (*Malurus melanocephalus*). Proceedings of the Royal Society B: Biological Sciences *287*, 20201687.
61. Twyman, H., Andersson, S., and Mundy, N.I. (2018). Evolution of CYP2J19, a gene involved in colour vision and red coloration in birds: Positive selection in the face of conservation and pleiotropy. BMC Evolutionary Biology *18*, 1–10.
62. Lopes, R.J., Johnson, J.D., Toomey, M.B., Ferreira, M.S., Araujo, P.M., Melo-Ferreira, J., Andersson, L., Hill, G.E., Corbo, J.C., and Carneiro, M. (2016). Genetic basis for red coloration in birds. Current Biology *26*, 1427–1434.
63. Kirschel, A.N.G., Nwankwo, E.C., Pierce, D.K., Lukhele, S.M., Moysi, M., Ogolowa, B.O., Hayes, S.C., Monadjem, A., and Brelsford, A. (2020). CYP2J19 mediates carotenoid colour introgression across a natural avian hybrid zone. Molecular Ecology *29*, 4970–4984.
64. Toews, D.P.L., Hofmeister, N.R., and Taylor, S.A. (2017). The Evolution and Genetics of

Carotenoid Processing in Animals. Trends in Genetics *33*, 171–182.
65. Price-Waldman, R., and Stoddard, M.C. (2021). Avian Coloration Genetics: Recent Advances and Emerging Questions. Journal of Heredity, 1–22.
66. Lamichhaney, S., Han, F., Webster, M.T., Andersson, L., Grant, B.R., and Grant, P.R. (2018). Rapid hybrid speciation in Darwin's finches. Science *359*, 224–228.
67. Abzhanov, A. (2009). Collection of Embryos from Darwin's Finches (Thraupidae, Passeriformes). Cold Spring Harbor Protocols *5*.
68. Picelli, S., Björklund, A.K., Reinius, B., Sagasser, S., Winberg, G., and Sandberg, R. (2014). Tn5 transposase and tagmentation procedures for massively scaled sequencing projects. Genome Research *24*, 2033–2040.
69. Li, H., and Durbin, R. (2010). Fast and accurate long-read alignment with Burrows-Wheeler transform. Bioinformatics *26*, 589–595.
70. Meisner, J., and Albrechtsen, A. (2018). Inferring population structure and admixture proportions in low-depth NGS data. Genetics *210*, 719–731.
71. R Core Team (2019). R: A Language and Environment for Statistical Computing.
72. Wickham, H., Averick, M., Bryan, J., Chang, W., McGowan, L., François, R., Grolemund, G., Hayes, A., Henry, L., Hester, J., et al. (2019). Welcome to the Tidyverse. Journal of Open Source Software *4*, 1686.
73. Lamichhaney, S., Han, F., Berglund, J., Wang, C., Almen, M.S., Webster, M.T., Grant, B.R., Grant, P.R., and Andersson, L. (2016). A beak size locus in Darwins finches facilitated character displacement during a drought. Science *352*, 470–474.
74. Poplin, R., Ruano-Rubio, V., DePristo, M.A., Fennell, T.J., Carneiro, M.O., Auwera, G.A. Van der, Kling, D.E., Gauthier, L.D., Levy-Moonshine, A., Roazen, D., et al. (2017). Scaling accurate genetic variant discovery to tens of thousands of samples. preprint at: https://www.biorxiv.org/content/10.1101/201178v3, 201178.
75. Paradis, E., and Schliep, K. (2019). Ape 5.0: An environment for modern phylogenetics and evolutionary analyses in R. Bioinformatics *35*, 526–528.
76. Yu, G. (2020). Using ggtree to visualize data on tree-like structures. Current Protocols in Bioinformatics *69*, 1–18.
77. Yu, G., Lam, T.T.Y., Zhu, H., and Guan, Y. (2018). Two methods for mapping and visualizing associated data on phylogeny using GGTree. Molecular Biology and Evolution *35*, 3041–3043.
78. Martin, M. (2011). Cutadapt removes adapter sequences from high-throughput sequencing reads. EMBnet.journal *17*, 10.
79. Pertea, M., Kim, D., Pertea, G.M., Leek, J.T., and Salzberg, S.L. (2016). Transcript-level expression analysis of RNA-seq experiments with HISAT, StringTie and Ballgown. Nature Protocols *11*, 1650–1667.
80. Alexaki, A., Kames, J., Holcomb, D.D., Athey, J., Santana-Quintero, L. V., Lam, P.V.N., Hamasaki-Katagiri, N., Osipova, E., Simonyan, V., Bar, H., et al. (2019). Codon and Codon-Pair Usage Tables (CoCoPUTs): Facilitating genetic variation analyses and recombinant gene design. Journal of Molecular Biology *431*, 2434–2441.
81. Lüdecke, D. (2021). sjPlot: Data Visualization for Statistics in Social Science.
82. Kuznetsova, A., Brockhoff, P.B., and Christensen, R.H.B. (2017). lmerTest Package: tests in linear mixed effects models. Journal of Statistical Software *82*.
83. Fox, J., and Weisberg, S. (2011). An {R} Companion to Applied Regression, Second Edition (SAGE publications).

888

KEY RESOURCES TABLE

REAGENT or RESOURCE	SOURCE	IDENTIFIER
Biological Samples		
Darwin's finch blood samples	This paper	https://github.com/erikenbody/Finch_beak_colo
Chemicals, Peptides, and Recombinant Proteins		
Tn5 Transposon	Karolinska Institutet Protein Science Facility	Addgene #79107
Critical Commercial Assays		
TaqMan Assay	ThermoFisher Scientific	Cat#: 4316034
Kapa Biosystems HiFi HotStart	Roche	Cat#: 7958927001
NEBNext Ultra RNA Library Prep Kit	New England Biolabs	Cat#: E7530L
E.Z.N.A. Total RNA Kit I	Omega Bio-Tek	R6834-01
Deposited Data		
Darwin's finch resequencing data	This project	PRJNA678752
Darwin's finch resequencing data (high depth)	64	PRJNA392917
Darwin's finch resequencing data (high depth)	46	PRJNA263122
Darwin's finch resequencing data (high depth)	71	PRJNA301892
Camarhynchus_parvulus_V1.1 reference genome	Rubin and Enbody et al. *in prep*	GCA_902806625.1
Darwin's finch phylogeny	46	21803
Oligonucleotides		
Tn5MErev, 59-[phos]CTG TCTCTTATACACATCT-39	66	
Tn5ME-A (Illumina FC-121-1030), 59-TCGTCGGCAGCGTCAGATGTGTATAAGAGACAG-39	66	
Tn5ME- B (Illumina FC-121-1031), 59-GTCTCGTGGGCTCGGAGATGTGTA TAAGAGACAG-39	66	
BCO2_F: 5'-TGTTTCAGAACCCAGTGACAACT-3'	This study	
BCO2_R:5'-TTCCAGTGTCTCTGGGTCCA-3'	This study	
BCO2_VIC:5'-ATGTGAACTACGTGCTGTAC-3'	This study	
BCO2_FAM:5'-ATGTGAACTACGTACTGTAC-3'	This study	
5'- CCCATCCCAGCCAAGATCAA-3'	This study	
5'- CGTAGTGGGGATGAGCTGTG-3'	This study	
BCO2_F2 - GCCACAACCCAGTGACAACT	This study	
BCO2_R1 - TTCCAGTGTCTCTGGGTCCA	This study	
Software and Algorithms		
BWA mem v0.7.17	67	

SAMTOOLS v1.10	http://www.htslib.org/	
ANGSD v0.935-33-g79d9455	17	
PCAngsd v1.01	68	
R v4.0.3	69	
Tidyverse R packages	70	
GATK v4.1.4.1	72	
BCFtools v1.10	http://www.htslib.org/	
Ape R package	73	
ggtree R package	74	
CutAdapt v.1.9	76	
Trim Galore v.0.4.1	http://www.bioinformatics.babraham.ac.uk/projects/trim_galore/	
HISAT2 v. 2.1.0	77	
StringTie v1.3.6	77	
Ballgown v2.20.0	77	
lmerTest R package	80	
car R package	81	
sjPlot	79	

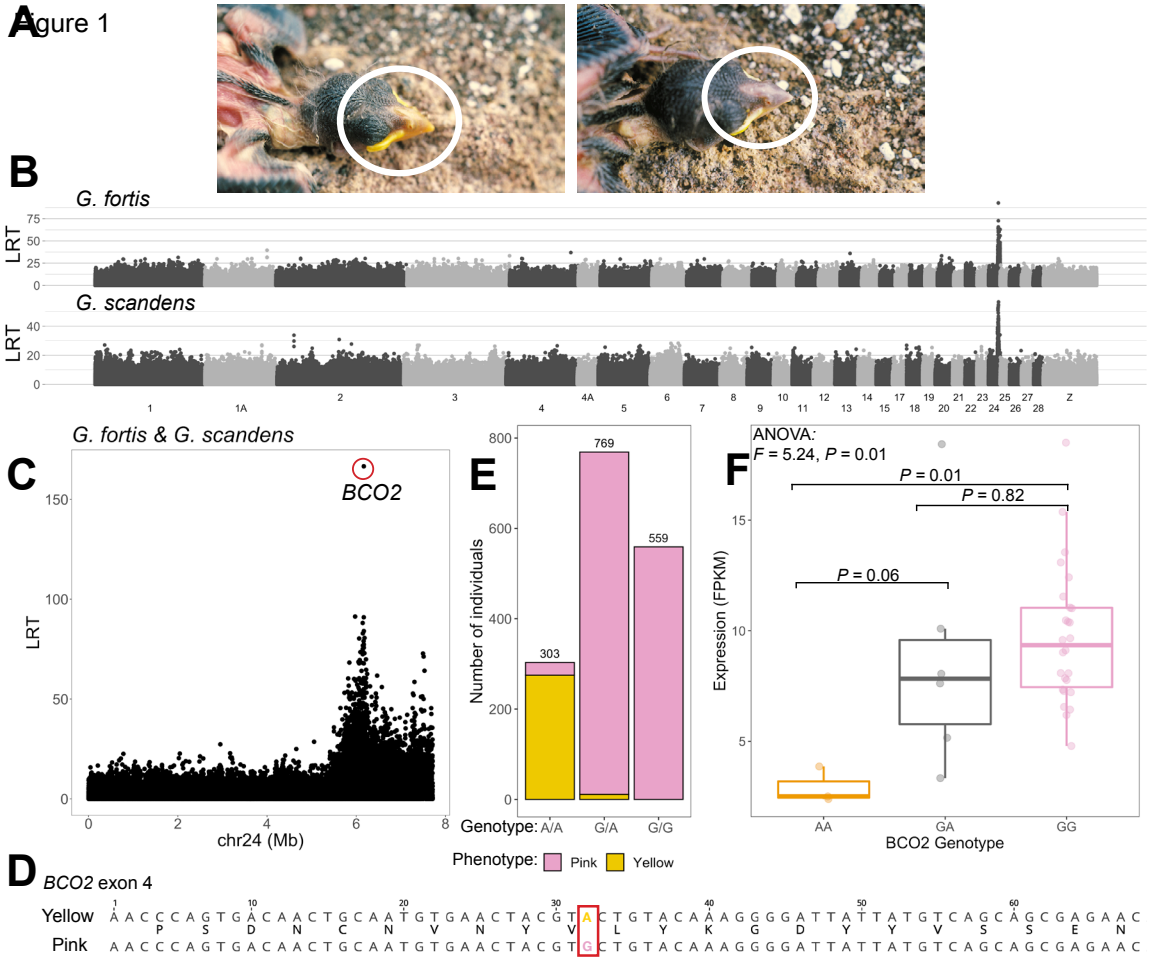
A
B
G. fortis
G. scandens
LRT
1 1A 2 3 4 4A 5 6 7 8 9 10 11 12 13 14 15 17 18 19 20 21 22 23 24 25 26 27 28 Z
C
G. fortis & G. scandens
BCO2
chr24 (Mb)
D
BCO2 exon 4
Yellow AACCCAGTGACAACTGCAATGTGAACTACGTACTGTACAAGGGGATTATTATGTCAGCAGCGAGAAC
Pink AACCCAGTGACAACTGCAATGTGAACTACGTGCTGTACAAAGGGGATTATTATGTCAGCAGCGAGAAC
E
Number of individuals
303
769
559
Genotype: A/A G/A G/G
Phenotype: Pink Yellow
F
ANOVA:
F = 5.24, P = 0.01
P = 0.01
P = 0.82
P = 0.06
Expression (FPKM)
AA GA GG
BCO2 Genotype

Figure 2

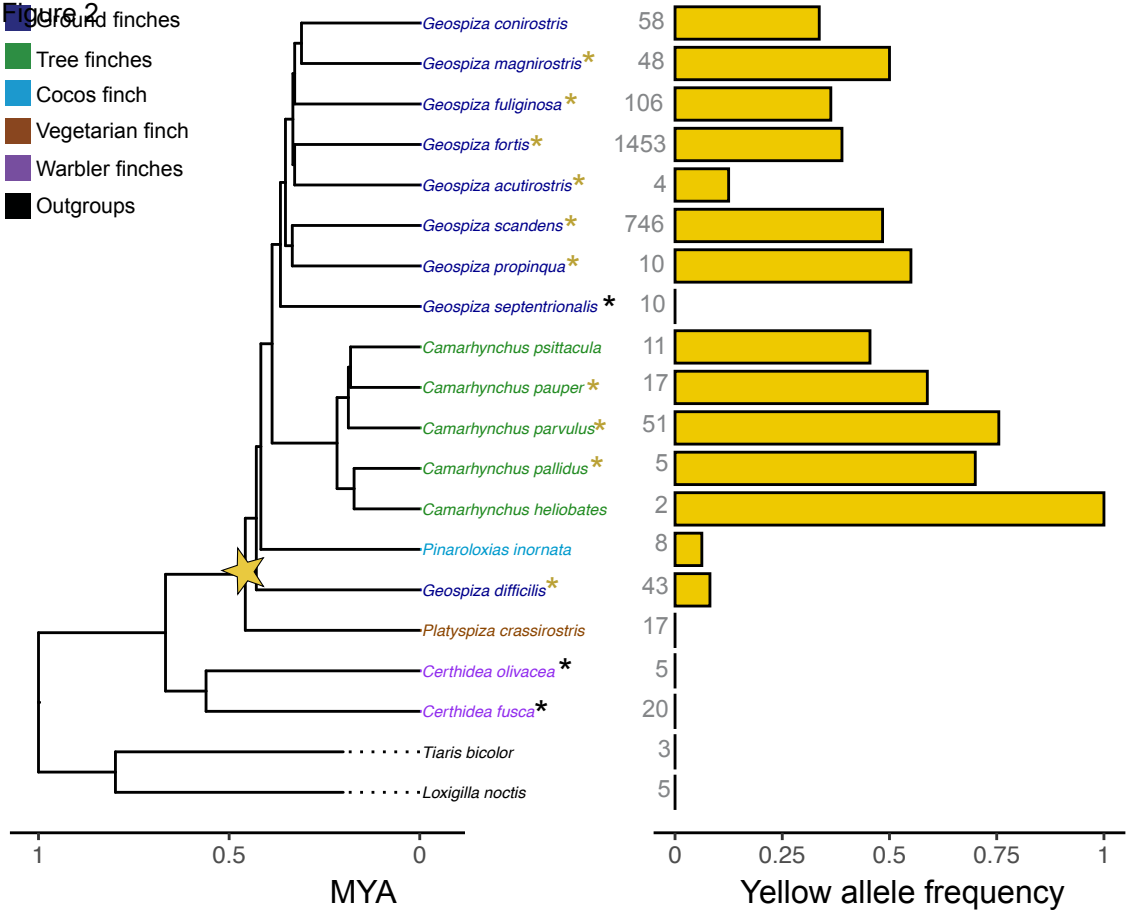
Ground finches
Tree finches
Cocos finch
Vegetarian finch
Warbler finches
Outgroups
Geospiza conirostris
Geospiza magnirostris
Geospiza fuliginosa
Geospiza fortis
Geospiza acutirostris
Geospiza scandens
Geospiza propinqua
Geospiza septentrionalis
Camarhynchus psittacula
Camarhynchus pauper
Camarhynchus parvulus
Camarhynchus pallidus
Camarhynchus heliobates
Pinaroloxias inornata
Geospiza difficilis
Platyspiza crassirostris
Certhidea olivacea
Certhidea fusca
Tiaris bicolor
Loxigilla noctis
58
48
106
1453
4
746
10
10
11
17
51
5
2
8
43
17
5
20
3
5
1
0.5
0
MYA
0
0.25
0.5
0.75
1
Yellow allele frequency

Figure 3

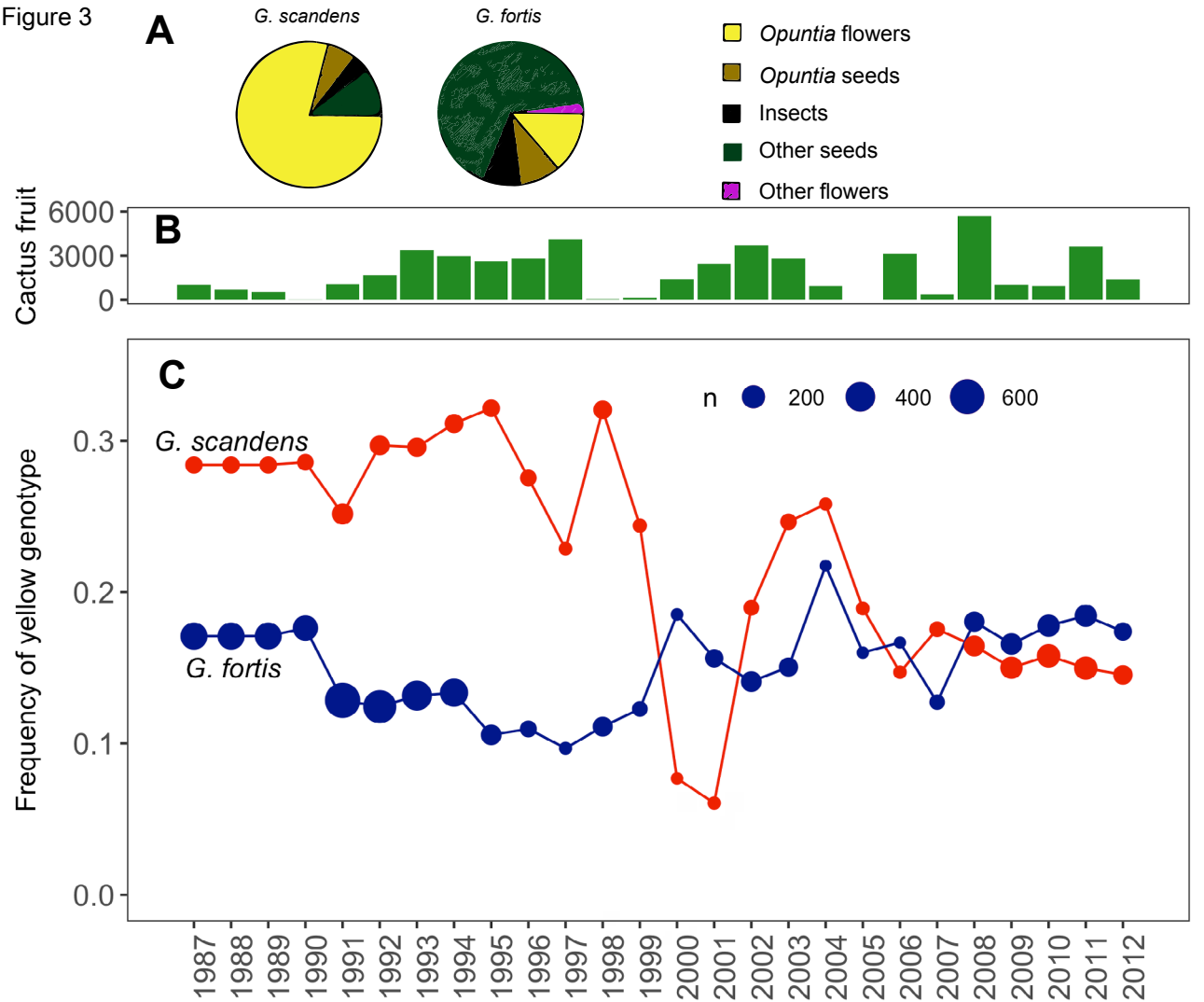
A
G. scandens
G. fortis
Opuntia flowers
Opuntia seeds
Insects
Other seeds
Other flowers
Cactus fruit
6000
3000
0
B
C
n
200
400
600
G. scandens
G. fortis
Frequency of yellow genotype
0.3
0.2
0.1
0.0
1987
1988
1989
1990
1991
1992
1993
1994
1995
1996
1997
1998
1999
2000
2001
2002
2003
2004
2005
2006
2007
2008
2009
2010
2011
2012

Figure 4

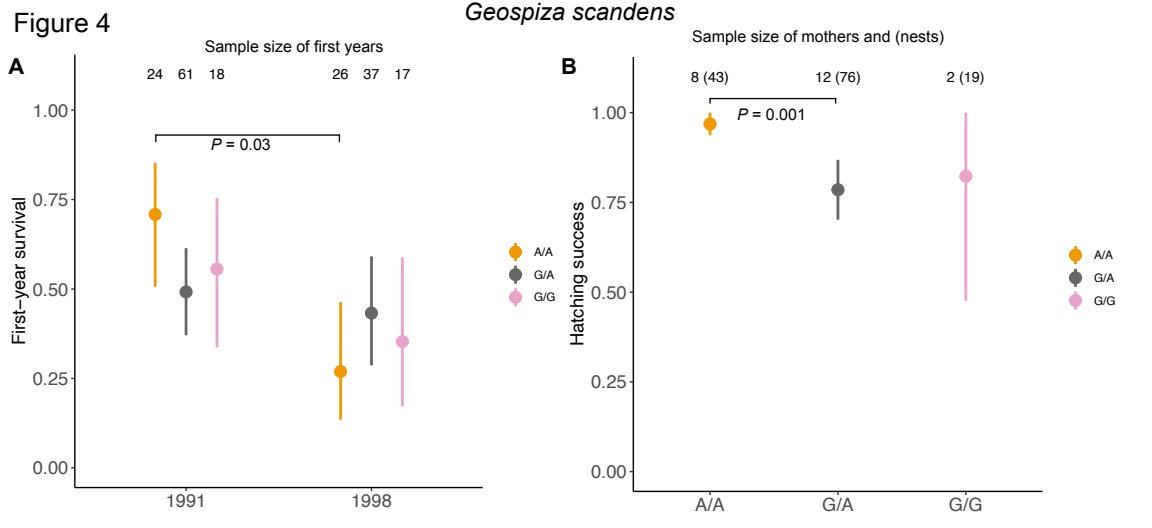
Geospiza scandens
A
Sample size of first years
24 61 18
26 37 17
P = 0.03
First−year survival
1.00
0.75
0.50
0.25
0.00
1991
1998
A/A
G/A
G/G
B
Sample size of mothers and (nests)
8 (43)
12 (76)
2 (19)
P = 0.001
Hatching success
1.00
0.75
0.50
0.25
0.00
A/A
G/A
G/G
A/A
G/A
G/G